

EVIDENCE FOR A FAST DECLINE IN THE PROGENITOR POPULATION OF GAMMA RAY BURSTS AND THE NATURE OF THEIR ORIGIN

B. E. STERN^{1,2,3}, J-L. ATTEIA⁴, K. HURLEY⁵

Draft version November 6, 2018

ABSTRACT

We show that the source population of long gamma-ray bursts (GRBs) has declined by at least a factor of 12 (at the 90% confidence level) since the early stages of the Universe ($z \sim 2 - 3$). This result has been obtained using the combined BATSE and *Ulysses* GRB brightness distribution and the detection of four GRBs with known redshifts brighter than 10^{52} erg s⁻¹ in the 50 - 300 keV range at their peak. The data indicate that the decline of the GRB source population is as fast as, or even faster than, the measured decline of the star formation rate. Models for the evolution of neutron star binaries predict a significantly larger number of apparently bright GRBs than observed. Thus our results give independent support to the hypernova model, which naturally explains the fast decline in the progenitor population.

Subject headings: gamma-rays: bursts – methods: data analysis

1. INTRODUCTION

The cosmological evolution of GRB progenitors at redshifts $z < 2$ can, in principle, reveal their nature. Indeed, we have unambiguous star formation data (hereafter SF; see Porciani & Madau 2001 and references therein) for the declining stage which started after $z \sim 2$, which we can use as a reference evolutionary curve. If GRB progenitors follow this curve or decline even faster than it, then we have to conclude that GRBs are most probably associated with the collapse of supermassive stars (hypernovae, or “failed supernovae” as originally suggested by Woosley 1993; see also Paczynski 1998 and MacFadyen & Woosley 1999). If the decline of GRBs is slower than the SF decrease then the coalescing neutron star binary model would be supported, as it naturally provides a delay between star formation and bursts.

GRB afterglow observations provide three lines of evidence in favor of the hypernova model as an explanation for the long duration GRBs. First, a large fraction of the afterglows are found near the central regions of their host galaxies (Bloom, Kulkarni & Djorgovski 2001). Second, features have been found in the light curves of three afterglows which can be interpreted as a supernova component (e.g. Bloom et al. 1999, Lazzati et al. 2001). And third, absorption features in some x-ray afterglow spectra (Galama & Wijers, 2001) and an emission iron $K\alpha$ line (Piro et al., 2000) indicate a high metal column density along the line of sight. For more details see the review of Meszaros (2001) and references therein. Although none of these facts constitutes a decisive argument by itself, together they strongly favor the hypernova model. However, the cosmological evolution of GRB sources can provide a new and completely independent test for the nature of GRB progenitors.

The problem of deriving the GRB source evolution from the data is not simple and cannot be solved by a straight-

forward cosmological fit to the log N - log P distribution with an unknown GRB luminosity function. Despite the wealth of statistics on GRBs accumulated by the Burst and Transient Source Experiment aboard the *Compton Gamma-Ray Observatory* (BATSE) (see Fishman et al. 1989), the bright end of the distribution still contains too few events to provide a conclusive χ^2 fit. For a review of cosmological fits to the log N - log P distribution see, e.g., Bulik (1999).

Stern, Tikhomirova & Svensson (2001 - hereafter STS), using the redshift data and the BATSE GRB sample, demonstrated the cosmological decline of GRB progenitors. A fast decline, similar to that of SF or even faster, was preferred by the data, but the statistics were insufficient to distinguish between the predictions of the hypernova and neutron star (NS) binary models at a significant level.

In this work we incorporate the data of the *Ulysses* GRB experiment, which more than double the number of strong GRBs and allow a more reliable interpretation of the redshift data. The main objective is to achieve a scientifically meaningful constraint on the NS binary model.

In §2 we describe the data and the procedure used to cross-calibrate the *Ulysses* and BATSE GRB samples. In §3 we outline the model fitting procedure, including the cosmological model, the parameterized luminosity function, and the GRB source evolution hypothesis. In §4 we present our results and show that the data require a very fast GRB progenitor decline, seriously challenging existing NS binary models.

2. THE DATA

We have used three independent data sets. The first contains 3255 BATSE GRBs with durations longer than 1 s, found by Stern et al. (2000, 2001) in the off-line scan of the 1.024 s time resolution BATSE continuous daily

¹Institute for Nuclear Research, Russian Academy of Sciences, Moscow 117312, Russia

²Astro Space Center of Lebedev Physical Institute, Moscow, Profsoyuznaya 84/32, 117810, Russia

³SCFAB, Stockholm Observatory, SE-106 91 Stockholm, Sweden

⁴CESR, 9, avenue du Colonel Roche, 31029 Toulouse Cedex, France

⁵University of California Space Sciences Laboratory, Berkeley, CA 94720-7450

records for the entire 9.1 yr BATSE mission⁶. This is the largest essentially uniform GRB sample, and its efficiency matrix has been measured using a test burst method. The second data set is the *Ulysses* sample, consisting of only bright GRBs, which are the most important ones for the aim of the present work. The *Ulysses* GRB detector has amassed well over 10 years of data to date, and since the detector is in interplanetary space and is neither Earth-nor spacecraft-occulted, it has $\approx 4\pi$ sr sky exposure and a larger effective duty cycle than BATSE (useful data are recovered for more than 95% of the mission), thus more than doubling the number of bright GRBs. The *Ulysses* GRB data on over 800 bursts have appeared in eight catalogs so far (Hurley et al. 1999a,b; Laros et al. 1997, 1998; Hurley et al., 2000a,b,c; Hurley et al. 2001a); the instrument description may be found in Hurley et al. (1992). The third data set consists of the GRB redshift data, or more specifically the data on the four intrinsically brightest events out of 23 GRBs with measured redshifts (up to November 2001)⁷.

The first two data sets were combined to form a single log N - log P distribution, i.e. the number of events versus the *apparent* peak brightness, P_a , while the third data set was used to constrain the bright end of the hypothetical *intrinsic* peak brightness (P_i) distribution (the luminosity function).

2.1. The BATSE and Ulysses samples, their cross-calibration, and the joint log N - log P distribution

The BATSE sample includes 3255 “long” (duration > 1 s) GRBs selected from 3906 GRBs in the sample of Stern et al. (2001), with the requirement that the counts in the second highest time bin exceed 50% of the counts in the highest time bin. This sample corresponds to 9.1 years of GRO observations with an average exposure factor 0.47. The latter includes both Earth-blocking and the average duty cycle for useful 1.024 s continuous records.

The *Ulysses* sample covers 10.3 years (Dec 1990 - Feb 2001) which overlap the entire BATSE mission. The average exposure factor of the GRB experiment is ~ 0.96 . This includes data outages, as well as periods when the background was high due to solar proton events. The short events were removed from the sample using the same criterion that we applied to BATSE GRBs. The effective energy range of the *Ulysses* GRB detectors is $\approx 25 - 150$ keV, while the BATSE data used for this study are for the 50 - 300 keV band.

Although both the *Ulysses* GRB detector and BATSE have quasi-isotropic angular responses, a direct conversion of Ulysses counts to BATSE peak flux is not possible for several reasons. First, the responses of both experiments have a weak angular dependence. Second, they operate in different spectral bands. And third, they have different efficiencies as a function of energy. The only realistic way to construct a joint log N - log P distribution is to do a cross-calibration using joint *Ulysses* /BATSE events. There are 278 such GRBs down to the *Ulysses* cutoff adopted here of 100 counts s^{-1} above background (the average background rate is 480 counts s^{-1}). A scatter plot of the *Ulysses* count

rate versus BATSE flux is shown in figure 1.

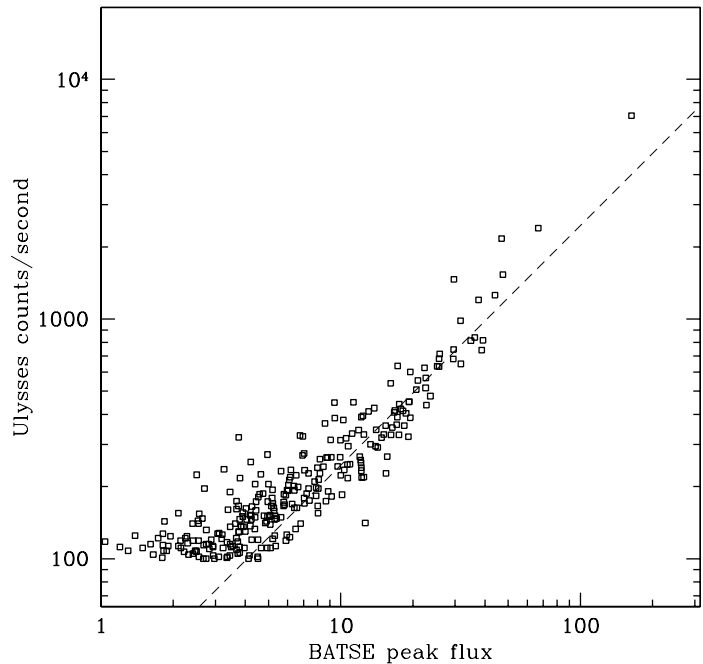


FIG. 1.— Ulysses count rate versus BATSE peak flux for 278 GRBs detected by both experiments. The sample has been truncated at a *Ulysses* peak count rate of 100 s^{-1} . The dashed line shows the ratio of the *Ulysses* count rate to BATSE flux, 24.6 cm^2 , which we use as the calibration coefficient.

The tendency towards higher Ulysses/BATSE ratios in the range below 10 photons $cm^{-2}s^{-1}$ is caused mainly by the Poisson bias (i.e., when one selects the highest Poisson fluctuation as a peak) and possibly by the hardness-brightness correlation in GRBs (see below). At the bright end of the distribution a similar bias is evident: the *Ulysses* count rates are again systematically higher. This is probably a saturation effect in the BATSE count rates, resulting from slow light emission in NaI scintillator (Meegan & Preece, 2001). This is probably a saturation effect in the BATSE count rates caused by dead time in the large BATSE detectors.

To avoid these biases we have restricted the analysis to bursts in the 10 - 40 photons $cm^{-2}s^{-1}$ range for the Ulysses/BATSE calibration. There are 73 events in this range; the average Ulysses/BATSE ratio is 24.6 cm^2 , and the rms variance is 5.2. The relatively large variance is due to the three reasons cited above. Note that this flux range gives the smallest *Ulysses* /BATSE ratio and therefore the largest values of *Ulysses* peak fluxes. Therefore it provides a conservative constraint on the decline of the GRB population.

In principle there should also be a brightness dependence in the *Ulysses* /BATSE ratio caused by the brightness-hardness correlation in GRBs (Nemiroff et al., 1994) and the different spectral bands and efficiencies as a function of energy. This effect may contribute to the tendency towards higher *Ulysses* /BATSE ratios for weaker GRBs (figure 1). We cannot separate this from the Pois-

⁶see http://www.astro.su.se/groups/head/grb_archive.html

⁷see, e.g., <http://www.aip.de/~jcg/grb.html>

son bias. However, Atteia (2001) parameterized the correlation between the *Ulysses* count rate and the 50 - 300 keV photon flux as $P_a \propto C_u^{1.14}$. Thus the brightness dependence is weak and has a negligible effect on the results. We prefer to use a constant calibration coefficient because there are insufficient data to quantify this dependence more accurately.

The joint BATSE-*Ulysses* log N - log P distribution is shown in figure 2. It includes 77 *Ulysses* bursts above $\log(P_a) = 1.2$. We chose this relatively high cutoff to conservatively avoid the Poisson bias in the *Ulysses* peak flux estimate. The number of BATSE GRBs in the range $\log(P_a) > 1.2$ is 43 (the total number of BATSE GRBs in the distribution is 3255).

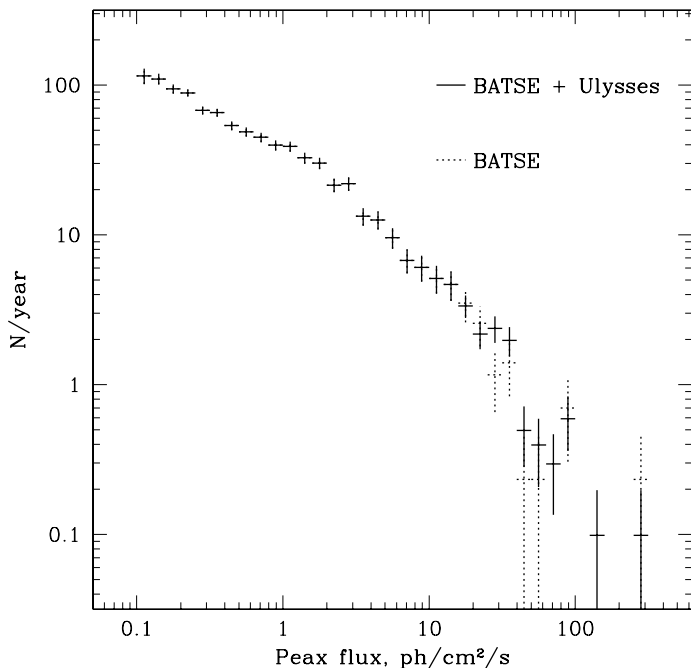


FIG. 2.— The joint BATSE - *Ulysses* log N - log P distribution.

The distribution below $\log(P_a) = 1.2$ is normalised to the total BATSE exposure, $9.1 \text{ yr} \times F_b$, where $F_b = 0.47$ is the BATSE exposure factor. The normalisation of points above $\log(P_a) = 1.2$ is the sum of the total BATSE/*Ulysses* exposure during 9.1 yr and the *Ulysses*-only exposure during 1.2 yr: $9.1 \text{ yr} \times (F_b + F_u - F_b \cdot F_u) + 1.2 \text{ yr} \times F_u$, where $F_u = 0.96$ is the *Ulysses* exposure factor.

2.2. The rate of intrinsically strong GRBs

The sample of events with known redshift is subject to strong selection biases and cannot be used directly to determine the luminosity function (see STS). It does, however, give useful information about the existence of intrinsically very bright GRBs. We can use this fact to constrain the bright end of the hypothetical luminosity function: the predicted rate of GRBs with P_i above some threshold at all redshifts should correspond to the observed rate. This constraint will affect the predicted number of apparently bright GRBs and therefore constrain the GRB source evolution model.

⁸see <http://www.asdc.asi.it/bepposax/>

For convenience we measure the intrinsic peak brightness P_i as the peak flux normalized to $z = 1$, taking the K-correction into account. The approximate relation between P_i and the isotropic peak 50 - 300 keV luminosity is $L = 3 \cdot 10^{50} \text{ erg s}^{-1} P_a$. STS have chosen the range $P_i > 40 \text{ photons s}^{-1} \text{ cm}^{-2}$ as a reference for the comparison between the hypothetical luminosity function and the data, and we use the same threshold here. Four of the intrinsically brightest bursts are above this threshold: GRB990123, GRB991216, GRB000131 and GRB010222, with redshifts of 1.6 (Djorgovski et al. 1999), 1.02 (Vreeswijk et al. 1999), 4.5 (Andersen et al. 2000), and 1.477 (Stanek et al. 2001) respectively; their apparent fluxes, P_a , in $\text{photons s}^{-1} \text{ cm}^{-2}$, are 16.4, 67.5, 6.3 (BATSE catalog) and 22.4 (*Ulysses* data with our *Ulysses*/BATSE calibration) respectively. Their P_i values are 45, 69, 84 and 48 $\text{photons s}^{-1} \text{ cm}^{-2}$, respectively.

These 4 events were detected over 4.2 years from the beginning of 1997 to March 2001. The latter date corresponds to the end of the processed *Ulysses* data that we use here (currently there are three GRBs with measured redshifts after March 2001).

The corresponding rate of GRBs at $P_i > 40 \text{ photons s}^{-1} \text{ cm}^{-2}$, I_{40} , multiplied by the probability that the burst will be detected and localized, its afterglow observed and its redshift measured (hereafter the sampling factor, F_s) is $0.95^{+0.60}_{-0.38}$. Now, in order to estimate I_{40} , we have to evaluate the sampling factor.

The first approach is simply to estimate F_s for *apparently* bright events, which would give a reasonable upper limit to the sampling factor for *intrinsically* bright events. Taking all *Ulysses* GRBs with peak count rates above 370 s^{-1} which corresponds to approximately $15 \text{ photons s}^{-1} \text{ cm}^{-2}$ (62 events from 1997 January 1 to 2001 March 1) we find redshift data for 4 of them (two of which are in the above list of four intrinsically bright GRBs). Using these numbers we estimate the sampling factor as $F_s \sim 0.064^{+0.038}_{-0.026}$. Taking the 1σ upper limit, 0.1, as a conservative estimate we obtain the rate of intrinsically bright GRBs $I_{40} \sim 10$.

The alternative approach is a direct estimate of the efficiency of the detectors used for burst localisations. 13 out of 23 redshift measurements were done using Beppo-SAX localizations. 7 of the remaining 10 bursts were localized by the Interplanetary Network (IPN: Hurley et al. 2001b). It is difficult to estimate the IPN efficiency, but the BeppoSAX efficiency has a well defined upper limit: the total field-of-view of the two Wide Field Cameras, ~ 0.08 of the sky⁸. Not every localisation, even of a strong burst, is followed by the observation of an afterglow and a redshift measurement. With this upper limit on the BeppoSAX efficiency and its share in the redshift sample we again obtain an estimate of the sampling factor of ~ 0.1 .

Therefore we adopt the estimate $I_{40} = 10/\text{yr}$ as our baseline and, to take the poor statistics into account, we also rederive all our results for $I_{40} = 4$. Future observations will show which value is closer to reality.

3. FITTING MODELS

The fitting model consists of three independent components: the cosmology, the evolution of the GRB source

population, and the intrinsic luminosity function (hereafter just luminosity function or LF).

The cosmological model is not very important for the purpose of the present work as it affects only large redshifts while the main issue we are concerned with here is the source evolution at low redshifts. We adopted a flat vacuum-dominated cosmology ($\Omega_\Lambda = 0.7, \Omega_M = 0.3$) which is supported by recent data (see, e.g., Lukash, 2000).

The evolution of the source population is the objective of our study. We tested four evolutionary functions. The first is a non-evolving population (NE). The second is the star formation function, which is a reasonable hypothesis for the evolution of GRB progenitors if they are collapsars. Porciani & Madau (2001) suggest three parameterized versions of the star formation rate which are very similar at small redshifts, but differ at large redshifts where the interpretation of the data is ambiguous due to the poorly known effects of dust absorption. Again, the evolution at large redshifts is beyond the scope of this work and we considered only one of these versions, namely:

$$R_{SF}(z) = \frac{0.15e^{3.4z}}{(e^{3.4z} + 22)} \text{ M}_\odot\text{yr}^{-1}\text{Mpc}^{-3} \quad (1)$$

This expression describes a constant SF rate at large redshifts and corresponds to a comoving volume.

The two other evolution functions used correspond to neutron star merger models. We obtained them by convolving the above SF rate with two different distributions for the delay between the formation of a binary system and the coalescence of its daughter neutron star binary. The first delay distribution was taken from Lipunov et al. (1995), hereafter L95, and the second from Portegies-Zwart & Yungelson (1998), hereafter PZY98. These distributions are quite different from one another. L95 predicts a peak at delays of 10 - 20 Myr and a long tail with a comparatively high probability of several Gyr delays. The distribution of PZY98 has a maximum around 1 Gyr and lower probability at several Gyr.

The standard candle log N - log P distributions for these four models are shown in Figure 3.

In addition to four fixed evolution models we tested different slopes of the decline phase of the source population, modifying Eq. (1) as

$$R_{SF}(z) \propto \frac{e^{1.086ln(a+1)z}}{(e^{1.086ln(a+1)z} + a)} \quad (2)$$

where a is a parameter describing the fall-off with redshift: $(a+1)$ is the ratio of the comoving rates of GRB emission at large z and at $z = 0$. The expression coincides with (1) at $a = 22$.

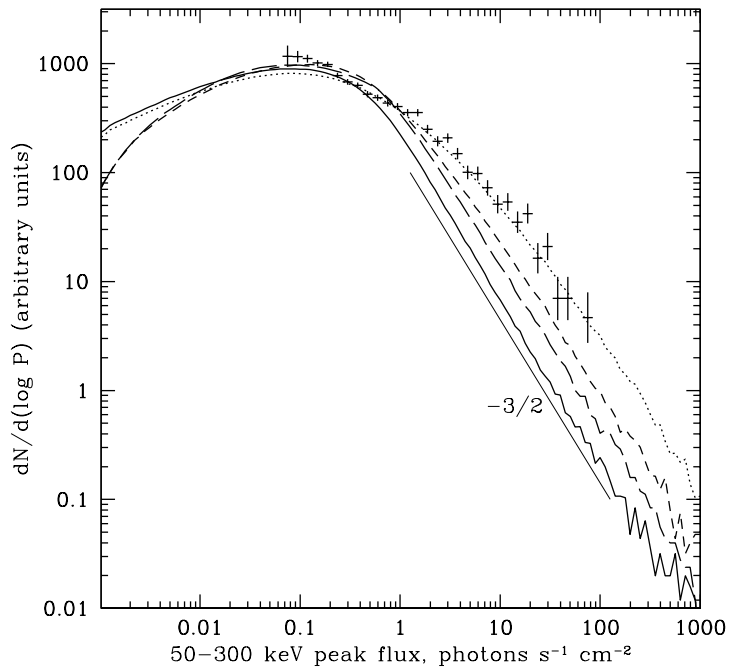


FIG. 3.— Standard candle log N - log P distributions for different models. The standard candle brightness corresponds to a peak flux of 1 photon $\text{s}^{-1} \text{cm}^{-2}$ at $z = 1$. Solid curve: SF model; dotted curve: NE model; dashed curve: SF model convolved with L95 delay function; dash-dotted curve: SF model convolved with PZY98 delay function. The crosses represent the observed log N - log P distribution of 3255 long BATSE GRBs. Theoretical curves are normalized to the same integral number of GRBs while data points are given in an arbitrary normalization.

The third component of the model is the hypothetical luminosity function. The data allow a wide choice with only two constraints: the width of the function, which must be at least 2.5 orders of magnitude (the luminosity range of GRBs with measured z), and the number of intrinsically bright GRBs (see section 2). We chose a broken power law, which proves sufficient freedom with a reasonably small number of free parameters:

$dN/dP = C \cdot P^{\alpha-1}$ for $P_1 < P < P_b$, $dN/dP = C_1 \cdot P^{\alpha+\beta-1}$ for $P_b < P < P_2$ and $dN/dP = 0$ beyond the interval $[P_1, P_2]$. The free parameters are α , β , P_1 , P_b , and C , while P_2 was fixed to a value above the maximum observed GRB brightness.

We used the forward folding method when fitting GRB data, i.e., the hypothetical brightness distribution was convolved with the efficiency matrix (1) and fitted to the observed differential log N - log P distribution (crosses in Figure 2) represented by 29 data points below $P = 50$ photons $\text{s}^{-1} \text{cm}^{-2}$. In 9.1 years of BATSE and *Ulysses* data, there were 15 GRBs brighter than this. We treat the range $P > 50$ photons $\text{s}^{-1} \text{cm}^{-2}$ separately, estimating the likelihood function of the fit for each peak flux range. For the main interval, this is the standard χ^2 probability function. For the tail of the brightness distribution, the likelihood is the Poisson probability of finding no more than 15 events apparently brighter than 50 photons $\text{s}^{-1} \text{cm}^{-2}$ assuming an average number A_{50} predicted by the model. The final likelihood function is the product of these two factors.

4. RESULTS

The best fit integral log N - log P distributions for the four models, SF, PZY98, L95, and NE are shown in figures 4 and 5.

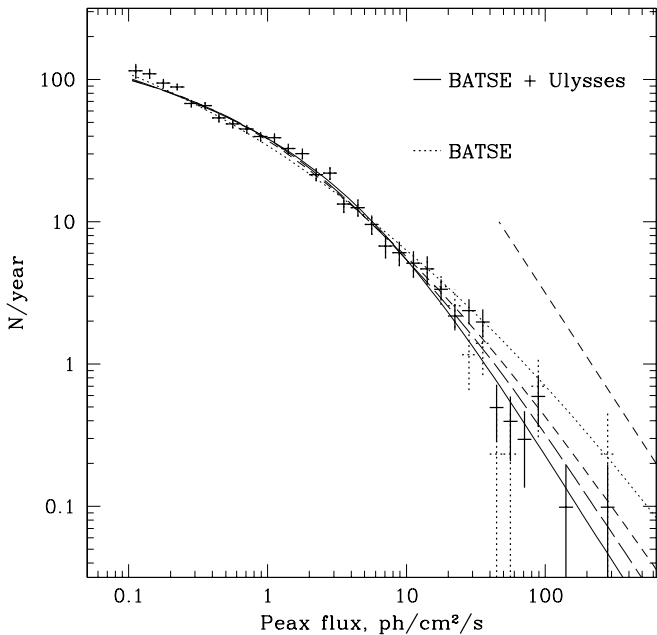


FIG. 4.— Comparison between the predictions of different evolutionary models and the data. Solid curve: SF; dotted curve: NE; dashed curve: L95; long dashed curve: PZY98; straight dashed line: the Euclidean $-3/2$ slope. Crosses are the observed data points, as in figure 2.

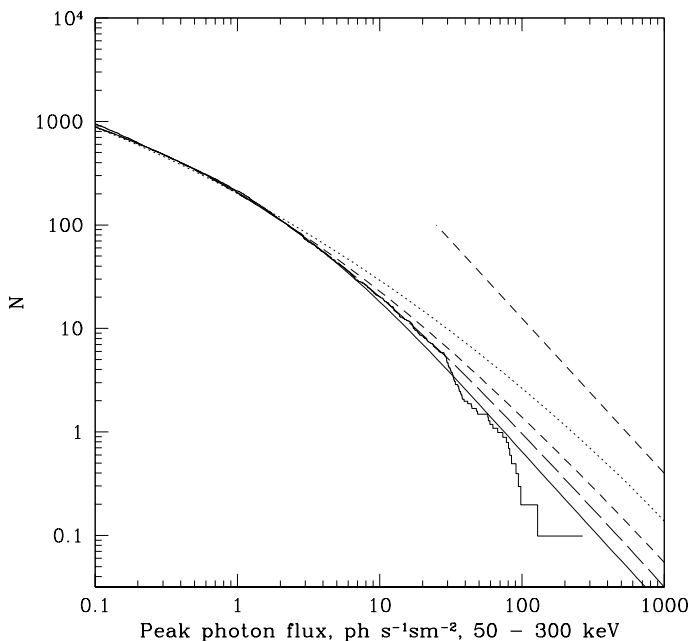


FIG. 5.— The same curves as in figure 4, but in integral form. Histogram - the integral peak flux distribution of *Ulysses*/BATSE GRBs. Solid curve: - SF model; dotted curve: NE; dashed curve: L95; long dashed curve: PZY98.

Adopting a rate of intrinsically bright GRBs $I_{40} = 10$,

their likelihoods are 0.034, $1.9 \cdot 10^{-3}$, $0.45 \cdot 10^{-5}$ and $2.2 \cdot 10^{-16}$ respectively. If we overestimate the rate of intrinsically strong GRBs by a factor 2.5 (assuming that 4 of the observed events with $P_I > 40$ are a fluctuation, so that $I_{40} = 4$, then the likelihoods are 0.40, 0.015, $0.95 \cdot 10^{-3}$, $2.65 \cdot 10^{-9}$ respectively.

Note that the rejection of the NE model (10^{-16}) is now much stronger than in STS (10^{-4}). This improvement is partially due to the better statistics of the joint BATSE-*Ulysses* sample, but mainly due to the fact that STS used too low an estimate for I_{40} : 3 events per year, inferred from the conservative assumption that $F_s \sim 0.5$ (compared to the present estimate $F_s \sim 0.1$ obtained using *Ulysses* data).

The sharp break in figure 5 around $P_a \sim 30$ photons $s^{-1} cm^{-2}$ is statistical in origin (note the corresponding deviation of the two data points in figure 4). This fluctuation is mainly due to the *Ulysses* sample; it is evident in Atteia et al. (1999).

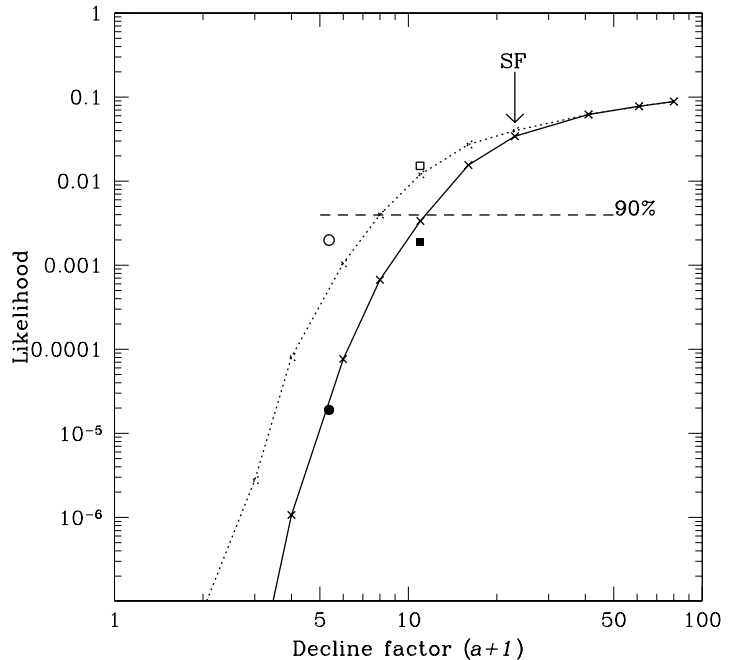


FIG. 6.— The likelihood versus the fall-off factor $(a+1)$ where a is the parameter in equation 2. The arrow shows the result for the SF model; the 90% confidence limit (dashed horizontal line) is given with respect to this model.

Figure 6 shows the likelihood factor for the parametrized source evolution model (equation 2) versus the fall-off factor $a+1$. The results for NS merger models are also shown; the ordinate for these models is just the ratio of the maximal NS merging rate (at $z \sim 2$) to that at $z = 0$. The likelihood curve has no turnover at large a because our luminosity function has only a lower limit constraint at its bright end. It is interesting that the curve still displays a considerable increase (by a factor of 2.6) from $a=22$, which corresponds to the SF curve, to $a = 80$, i.e., the data are better fit by a GRB progenitor fall-off which is faster than the SF rate. This could be a natural consequence if the progenitors are supermassive stars whose population can decline faster than the total SF. However, this indication is

statistically weak and could also result, for example, from the same fluctuation in the *Ulysses* data which produces a break in the log N - log P curve around 20 - 30 photons $\text{s}^{-1} \text{cm}^{-2}$, as discussed above.

More details of the fits are presented in Table 1, where χ^2 and the predictions for A_{50} are given separately. We do not present the best fit parameters for the broken power law luminosity function because they are consistent with the results of STS where this issue was studied in detail.

Table 1, as well as figures 4 and 5, clearly demonstrate that models with an insufficiently steep evolutionary decline of GRB progenitors predict an excess of apparently strong GRBs with respect to the observations.

Model	lkh	χ^2	A_{50}	lkh(A_{50})
NE	$2.2 \cdot 10^{-16}$	83	49	$1.28 \cdot 10^{-8}$
SF ₂₂	0.034	31	18.6	0.24
L85	$1.9 \cdot 10^{-5}$	37	33	$2.1 \cdot 10^{-4}$
PZY98	$1.9 \cdot 10^{-3}$	32	26	$1.4 \cdot 10^{-2}$
SF ₈₀	0.088	31	15	0.57
SF ₄₀	0.062	31	16	0.47
SF ₁₀	$0.36 \cdot 10^{-2}$	31	25	$2.2 \cdot 10^{-2}$
SF ₅	$0.76 \cdot 10^{-4}$	38	30	$1.9 \cdot 10^{-3}$

Table 1 The maximum likelihood results for various models. The second column (lkh) gives the final likelihood factor; the third column, the χ^2 value (at 24 degrees of freedom); the fourth, the predicted A_{50} (the observed A_{50} is 15); the fifth, the probability of observing A_{50} less than 16 for its predicted value. The subscripts in the first column correspond to the value of a (see equation 2). SF₂₂ in row 2 corresponds to the measured star formation curve.

If we use the Bayesian approach, treating the ratio of likelihoods as the relative probabilities of different models, then the rejection factors for NS models relative to SF are 0.055 for PZY98 and $1.3 \cdot 10^{-3}$ for L95. If we adopt the estimate $I_{40} = 4$ then the constraints relax to 0.37 and 0.024 respectively, i.e. the PZY98 model is consistent with the data. Note however that the choice of $I_{40} = 4$ corresponds to a less than 0.1 probability fluctuation in the number of intrinsically bright GRBs with measured redshifts.

The minimal fall-off factor allowed by the data at 90%

confidence level is $a + 1 \sim 12$ or $a + 1 \sim 8$ for $I_{40} = 4$.

5. CONCLUSIONS

The joint BATSE - *Ulysses* data confirm a sharp decline in the GRB source population between $z \sim 2$ and the present epoch. Although it is consistent with that of star formation, a faster decline is slightly preferable, albeit at a statistically insignificant level ($\sim 1\sigma$). The two models of binary system evolution leading to a final NS merger are well beyond the 90% confidence limit, except for the $I_{40} = 4$ case, which is based on the assumption of a large fluctuation in the observed number of intrinsically bright GRBs. Note that while the statistics of bright GRBs will improve slowly, the redshift statistics can improve much faster, so that a more reliable estimate of I_{40} may be available relatively soon.

The joint BATSE/*Ulysses* data present a new challenge to the neutron star binary model as an explanation of the source of long GRBs. Together with the results of afterglow studies it makes it very improbable. The only way to save the NS model is to show that the typical lifetimes of such systems is short. If very few survive longer than 1 Gyr, this will fit the log N - log P distribution, and if many merge in a few Myr, this will explain the locations of the observed afterglows in the star forming regions of their host galaxies. Such a possibility has been studied in the recent work of Belczynski, Bulik & Rudak (2001) where it is shown that this could occur in some binary evolution models due to common envelope events producing very tight NS systems. Finally it should be pointed out again that our constraints refer only to the class of long GRBs, while the NS binary model is probably able to explain the origin of short bursts.

We thank Ya.Tikhomirova for assistance. This research made use of data obtained through the HEASARC Online Service provided by NASA/GSFC. It was supported by the Swedish Natural Science Research Council, the Royal Swedish Academy of Science, the Wennergren Foundation for Scientific Research and the Russian Federation for Basic Research (grant 00-02-16135). KH is grateful for *Ulysses* support under JPL Contract 958056.

REFERENCES

- Andersen, M.I., et al. 2000, *A&A*, 364, L54
 Atteia, J.-L., Boer, M., & Hurley, K., 1999, *Astron. Astrophys. Suppl. Ser.* 138, 421
 Atteia, J.-L., Boer, M., & Hurley, K. 2001, in *Proc. of the 19th Texas Symposium on Relativistic Astrophysics and Cosmology*, Ed. J. Paul, T. Montmerle, & E. Aubourg (CEA Saclay), 4
 Atteia, J.-L., 2001, communication
 Belczynski, K., Bulik, T., & Rudak, B. 2001, astro-ph/0112122
 Bloom, J., et al. 1999, *Nature* 401, 453
 loom, J.S., Kulkarni, S.R., Djorgovski, S.G., 2001, *ApJ* in press, astro-ph/0010176
 Bulik, T. 1999, in *ASP Conf. Series 190, GRBs: The First Three Minutes*, ed. J. Poutanen, & R. Svensson (San Francisco: ASP), 219 (astro-ph/9911437)
 Djorgovski, S.G., et al. 1999, *GCN notice* 251
 Fishman, G. J., et al. 1989, in *Proc. of the Gamma Ray Observatory Science Workshop*, ed. W. N. Johnson (Greenbelt: GSFC), 3
 Galama, T., and Wijers, R. 2001, *Ap. J.* 549, L209
 Hurley, K., et al. 1992, *Astron. Astrophys. Suppl. Ser.*, 92(2), 401
 Hurley, K., et al. 1999a, *ApJS* 120, 399
 Hurley, K., et al. 1999b, *ApJS* 122, 497
 Hurley, K., et al. 2000a, *ApJS* 533, 884
 Hurley, K., et al. 2000b, *ApJS* 534, 258
 Hurley, K., et al. 2000c, *ApJS* 128, 549
 Hurley, K., et al. 2001a, in preparation
 Hurley, K., et al. 2001b, in *Gamma-Ray Bursts in the Afterglow Era*, Eds. E. Costa, F. Frontera, and J. Hjorth, *ESO Astrophysics Symposia*, Springer (Berlin), p.378
 Laros, J., et al. 1997, *ApJS* 110, 157
 Laros, J., et al. 1998, *ApJS* 118, 391
 azzati, D., et al., 2001, *Astron. Astrophys.* in press, astro-ph/0109287
 Lipunov, V. M., Postnov, K. A., Prokhorov, M. E., Panchenko, I. E., Jorgensen, H. E., 1995, *ApJ*, 454, L363
 Lukash, V. N. 2000, astro-ph/0012012
 MacFadyen, A., and Woosley, S., 1999, *Ap. J.* 524, 262
 Meegan, C., Preece, R., 2001, *Communication*
 Meszaros, P., 2002, in press *Annu. Rev. Astron. Astrophys.* 40, astro-ph/0111170
 Nemiroff, R., et al. 1994, *Ap. J.* 435, L133
 Paczynski, B., 1998, *Ap. J.* 494, L45
 Piro, L., et al., 2000, *Science*, 290, 955
 Porciani, C., & Madau, P. 2001, *ApJ*, 548, 522
 Protegias-Zwart, S.F., Yungelson, L.R., 1998, *A&A*, 332, 173
 Stern, B. E., Tikhomirova, Ya., Stepanov, M., Kompaneets, D., Berezhnoy, A., & Svensson, R. 2000, *ApJ*, 540, L21
 Stern, B. E., Tikhomirova, Ya., Kompaneets, D., Svensson, R., & Poutanen, J. 2001, *ApJ*, 563, 80
 Stern, B. E., Tikhomirova, Ya., and Svensson, R., 2002, *ApJ*, in press, (astro-ph/0108303)

Vreeswijk, P. M., et al. 1999, GCN notice 496

Woosley, S., 1993, ApJ, 405, 273